Journal of Alloys and Compounds 509 (2011) 2874–2878

Contents lists available at ScienceDirect

Journal of Alloys and Compounds

journal homepage: www.elsevier.com/locate/jallcom

Facile synthesis of highly oriented p-type aluminum co-doped zinc oxide film with aqua ammonia

Ian Y.Y. Bu*

Department of Microelectronics Engineering, National Kaohsiung Marine University, No. 142, Haijhuan Road, 81157 Nanzih District, Kaohsiung City, Taiwan, ROC

ARTICLE INFO

Article history:
Received 20 August 2010
Received in revised form
16 November 2010
Accepted 22 November 2010
Available online 30 November 2010

Keywords:
P-type
Zinc oxide
Sol–gel
Highly oriented
Co-doping

ABSTRACT

Zinc oxide (ZnO) is a wide band-gap material with excellent optoelectronic properties. However, the application of ZnO to optoelectronic devices using ZnO has been hindered by the difficulty in obtaining a stable p-type doping. The paper demonstrates that, with a proper selection of the nitrogen precursor, a solution processable, highly *c*-axis oriented, stable, and p-type aluminium co-doped ZnO (NZO) formation can be obtained. In this study, the NZO films were characterized by using EDS, Raman spectroscopy, photoluminescence, and electrical measurements, respectively. The films were then synthesized through a sol–gel process that was below 600 °C. For the comparative study, NZO films without the Al co-doping were also prepared by sputter. It is observed and shown that, with the formation of nitrous oxide, the basic deposition condition will be more beneficial towards the formation of p-type ZnO.

1. Introduction

ZnO is a direct wide band-gap (Eg = 3.4 eV) semiconducting material, with a large exciton binding energy (60 meV) and possess good transparency in the visible wavelength [1]. The synthesis of a wide range of ZnO nanostructures has recently attracted considerable research interests (e.g., nanowires [2,3] and nanoflowers [4]). The potential applications of ZnO nanostructures include, solar cells [5,6], gas sensors [7–9], nanostructured transparent conductive oxide (TCO) [10] and bio-related applications [11]. The effective and reliable creation of the p-type ZnO plays a crucial part in the advancement of ZnO for optoelectronic device applications. However, it is difficult to produce p-type ZnO due to the low solubility of acceptor dopants in ZnO, the excessive accepter ionization energy, and the compensating mechanisms [12].

To date, two strategies have been developed to synthesis p-type ZnO: (1) Direct doping through substituting either group I elements such as Na [13], K [14] or Li [15] with Zn, or group V elements such as N [16], P [17], As [18] or Sb [19] for oxygen, (2) co-doping with N or Li acceptor with reactive donors such as Ga, In or Al [20–22].

The direct doping method substitutes either zinc by Group I elements, Na [13], K [14], Li [15], or oxygen by Group V elements, N [16], P [17], As [18], and Sb [19]. It has been reported by Tay [14] that, in the direct doping method, N possesses the most compatible bond length whilst Li has the shallowest ionization energy. Further more, Wang et al. [23] observed that the incorporation of Li into crystal lattices, rather than into grain boundaries, can achieve a superior electrical performance. Their study also revealed that the deposition condition can have considerable influence on the electrical properties of the film. Additionally, hydrogen also plays an important role in the direct doping process because the diffusion of H impurities in the films can cause the transition from p-type to n-type conduction mechanism [12].

The co-doping method utilizes the reactive donors (Ga, In, and Al [20–22]) to the acceptor (N or Li). The dual doping with the combination of N and Li has also been studied [24]. Two distinct advantages of the N/Al combination are the material abundance and the greater acceptance by the semiconductor manufacturers. Nitrogen doped p-type zinc oxide (NZO) has also been developed by various research groups, by using different techniques, such as, CVD [25,26], sol–gel [27], sputtering [28–30] and evaporation [31,32]. In these techniques, the p-type dopant was achieved by adding N as the co-dopant, with or without Al [31,28].

Compared to the conventional methods, such as sputtering, the sol–gel method has several advantages; for example, using simple equipments, the precise control of film composition, a large-area capability and high material utilisation. However, few studies on the sol–gel synthesis of p-type NZO are available in the literature. Dutta et al. [33] obtained a stable and conductive p-type NZO by co-doping of N with Al through sol–gel process, without investigating the effects of chemical compounds selection on the property of NZO. Indeed, the published results from the sol–gel synthesis of

* Tel.: +886 972506900; fax: +886 73645589.
E-mail address: ianbu@hotmail.com

0925-8388/$ – see front matter © 2010 Elsevier B.V. All rights reserved.
doi:10.1016/j.jallcom.2010.11.146

ZnO-related films have confirmed that the chemical compounds selection has a significant effect on the structure, optical and electrical properties of the film [34]. Copuroglu et al. [35] showed that the combination of monoethanolamine (MEA) with alcohol can lower the crystallization temperature of aluminium doped zinc oxide (AZO) and create highly *c*-axis oriented films [35].

This paper adopts different nitrogen-containing chemicals as the dopant source in order to study the mechanism of p-type NZO formation. The p-type ZnO:Al:N (NZO) films had been synthesised by the sol–gel process, using isopropanol (IPA), MEA, aluminium chloride ($AlCl_3$) with ammonia chloride (NH_4Cl), and aqua ammonia (NH_4OH). The nitrogen doped ZnO without Al co-doping and the sputter coated ZnO:Al:N were also synthesised respectively. The film's electrical, optical and structural properties were measured by using Hall's measurement, X-ray diffraction, Raman spectroscopy and scanning electron microscopy (SEM). Based on the investigation results, the influences of the selection of nitrogen sources on the film's properties were identified and discussed.

2. Materials and methods

The preparation of samples for the sol–gel and sputtered methods, respectively, is described in this section. Corning Eagle 2000 glass and low doped, n-type, double-side polished crystalline silicon substrates have been used for sample characterisation. Substrates were cleaned prior to deposition by immersing consecutively in ultrasonic baths of acetone, isopropanol and deionised water. The silicon substrates were then dipped in buffered hydrofluoric acid in order to remove any native silicon oxide on the surface.

In order to conduct a comparative study, four samples were prepared: namely NZO (synthesised by NH_4Cl and Al), NZO (synthesised by NH_4OH with Al), sputtered NZO (with a Zn/Al target in nitrogen environment) and NZO (synthesised by NH_4OH without Al).

Sol was prepared by mixing of 0.7 M zinc acetate ($Zn(CH_3COO)_2{\cdot}H_2O$) (Sigma–Aldrich) in isopropanol IPA (Sigma–Aldrich), with an equal molar ratio of MEA added as a stabilizer to prevent precipitation (see supporting information). The solution was magnetically stirred at 70 °C for 1 h until a clear solution was formed. All the sols were then left to age for one day in a sealed vessel. The prepared solutions were found to be stable for months and transparent with no precipitation.

NH_4Cl (0.03 M) and NH_4OH were selected as the nitrogen source, respectively, and the co-doping was achieved by adding 1 wt% $AlCl_3$ into the sols. For comparison purposes, a sample without Al co-doping and sputter coated NZO was also synthesized. Depositions were performed in atmospheric air and spin coated at 3000 rpm for 30 s. It should be noted that the boiling points for MEA and IPA were 170 °C and 82.5 °C respectively. As a result, films were first heated to 250 °C, in order to ensure a complete evaporation of the solvents, and subsequently sintered to 550 °C by a hotplate to crystallize the films. The deposition thickness of the NZO films was controlled by the repetition of spin-dried cycle.

Commercially available aluminium doped zinc oxide disc (2 in. in diameter, 3 mm thick) was also used in the comparative study. The sputter target was cleaned by the Ar plasma at 100 W for 15 min before deposition. The deposition condition was at a power of 100 W, base pressure = 7×10^{-6} Torr, working pressure of 8×10^{-3} Torr within a gas mixture of Ar/N_2 of 100:100 at 275 °C. The sample was characterised without post annealing.

The SEM images of the sol–gel derived films were taken by using a FEI Quanta 400 F Environmental Scanning Electron Microscope (ESEM). Energy dispersive spectroscopy (EDS) was also conducted in the same chamber. The crystal orientation was investigated by using a Siemens D5000 X-ray Diffractometer using Cu Kα radiation. Raman spectroscopy of the NZO films was performed by using a Dongwoo Macro Raman spectrometer. The Hall measurements were taken by a four-point probe in Van der Pauw configuration to determine resistivity and carrier concentration. Contacts were sputtered on the four corner of the sample to ensure low contact resistances. The photoluminescence (PL) measurements were performed by a 325 nm He/Cd laser (Jasco Model FP-6000).

3. Results and discussion

Fig. 1(a)–(e) presents the SEM images of surface morphology of the NZO films doped with different nitrogen sources, respectively, on a Corning glass substrates. The NZO films on glass are composed of compacted and dense nanoparticles with diameters in the range of 10–50 nm. Whilst Fig. 1(a) shows the SEM of the films on a macroscopic level (5 μm scale), Fig. 1(b)–(e) shows the SEM at a higher resolution.

In general, the NZO produced by the sol–gel method possesses a wrinkled thin film embedded within the smaller grain ZnO particles. Furthermore, the sol–gel NZO films derived without Al co-doping (Fig. 1(b)) by using NH_4Cl (Fig. 1(c)) and NH_4OH (Fig. 1(d)) exhibit a wrinkle-network on the surfaces. The "wrinkle" phenomenon has been studied by other research groups [36,37] and is considered usually caused by stress relaxation during the sintering of the ZnO films. The wrinkle phenomenon is only visible on a macroscopic level (5 μm scale), as given in Fig. 1(a). As expected, the sputtered film does not show any wrinkle phenomenon. It should be noted that the sputtered film, presented in Fig. 1(e), has a relatively larger grain size. The grain size of ZnO films is highly influenced by the synthesis/annealing temperature [38]. As the sputtered film was derived from a sputtering target sintered at a much higher temperature, the density and grain size of ZnO increases accordingly [39].

Fig. 2 presents the XRD patterns of the synthesized NZO films. It is important to note that, all the films have shown preference orientation along the (0 0 2) plane. The films consist of ZnO crystals that show a preference to the *c*-axis. Generally, the broadness of the XRD peaks is an indication of the degree of crystallinity. As expected, the sputtered ZnO:Al:N showed a broad peak which confirmed the amorphous structure of the film. As illustrated in Fig. 2, the XRD pattern for ZnO:Al:N is very sensitive to the chemical source selection. The films derived from NH_4Cl have produced a weaker XRD signal intensity than those from NH_4OH. These results are significant and indicate that the orientation and quality of p-type ZnO films that can be effectively controlled through chemistry properties of the sol. Clearly, the utilisation of NH_4OH can produce a better quality crystalline film with an extreme preference to the *c*-axis. The average crystallite size was estimated by Scherrer's formula

$$d = \frac{0.9\lambda}{B \cos \theta_B}$$

where λ is the X-ray wavelength of 1.54 Å, θ_B is the Bragg diffraction angle and *B* is the FWHM (full width at half maximum) of θ_B. The estimated average sizes are tabulated in Table 1. The crystallite information extracted from XRD does not correlate with data from SEM given in Fig. 1. This can be explained by the fact that XRD measurements are likely to underestimate the mean grain size. The under estimation is caused not only by instrumental broadening of FWHM but also by stress-induced broadening [40].

Fig. 3 shows the elemental film composition analysis determined by EDX. The EDX data confirms that the films consist of Al, Zn, O and N. The N concentration of the films was 2.16% (sol–gel synthesized NZO without Al doping), 3.04% (sputtered ZnO:Al:N), 2.77% (sol–gel produced ZnO:Al:N, using NH_4Cl as the source), and 1.36% (sol–gel produced ZnO:Al:N using NH_4OH as the source). These nitrogen contents were reasonably close to the intended 3%. The EDX data also shows that the sputtered film had incorporated most nitrogen and the ZnO:Al:N (NH_4OH) the least. Dutta et al. [33] has suggested that NH_3 readily escapes from ammoniac solution, unless the experiment is conducted under airtight condition. During the sputtering process, the chamber had been evacuated into high vacuum (10^{-6} Torr). The nitrogen gas was injected into the chamber, broken into atomic nitrogen and incorporated into the films. The films deposited under nitrogen filled environment, should have incorporated higher nitrogen content within the film.

During the sol–gel process for the ZnO production, several reactions can occur. The reaction for NZO is proposed as follows. Zinc acetate dehydrate was mixed with IPA and stabilized with MEA to produce H ions and OH ions. The hydrolysis of zinc acetate (saponification) leads to acetic acid and an OH– ion. It is noted that hydrolysis of the precursor is an important step in the sol–gel

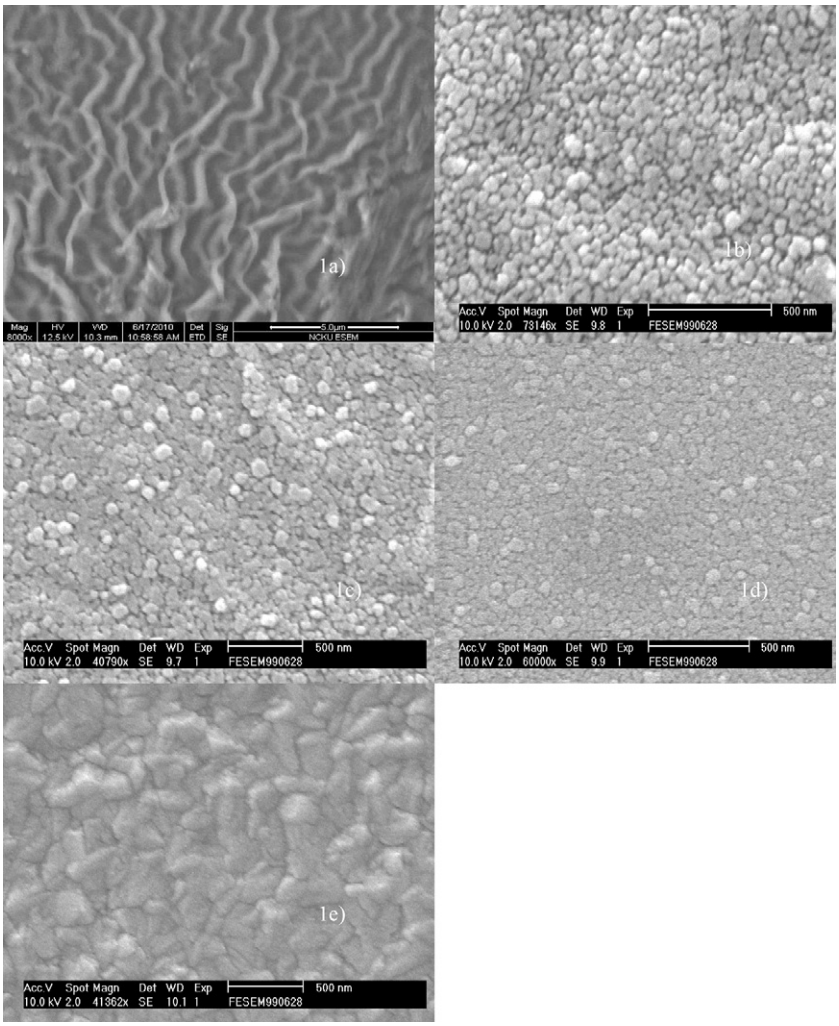

Fig. 1. SEM image. (a) Typical sol–gel derived NZO film at lower magnification, (b) sol–gel synthesized NZO without Al co-doping, (c) sol–gel produced ZnO:Al:N using NH_4Cl as source of nitrogen, (d) sol–gel produced ZnO:Al:N using NH_4OH as source and (e) sputter coated ZnO:Al:N.

production of zinc oxide. A previous study [35] observed an opto-electronics degradation of the films when anhydrous zinc acetate was used as the source with water excluded from the experiment. The zinc acetate transforms into mono-acetate Zn in IPA. The source of water molecules can be from the solution or air. As the sol is heated over 80 °C, IPA evaporates from the film. The H and OH ions convert zinc acetate into $Zn(OH)_2$ which can be further broken down into ZnO and water. In the case of NH_4Cl addition, which is mildly acidic, the H and Cl had combined to form HCl. HCl is a known etchant for ZnO and is often used to create a texturized ZnO films for TCOs [41]. This result is also reflected in the EDX elemental study, where ZnO has slightly less zinc content than other samples, indicating wet etch of oxide has occurred. In the case of NZO (NH_4OH), the additional OH aids the formation of NO and OH, which is beneficial towards the formation of NZO, with superior *c*-axis preference. In summary, the important finding is that basic

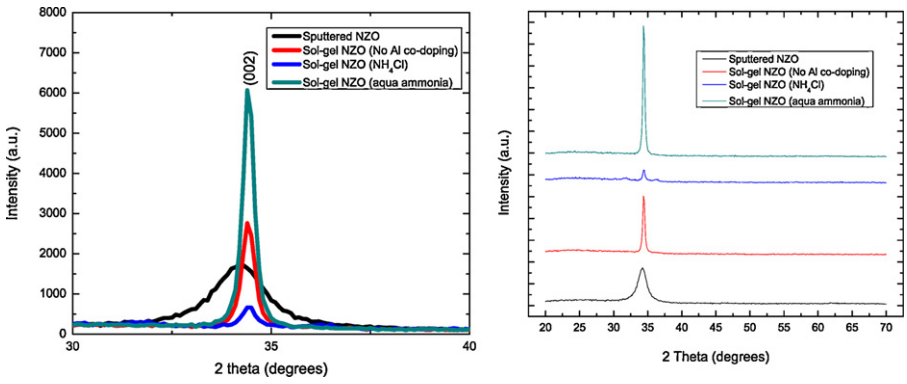

Fig. 2. XRD of the synthesized NZO films, sol–gel synthesized AZO, sol–gel produced ZnO:Al:N using NH_4Cl as source of nitrogen, sol–gel produced ZnO:Al:N using NH_4OH as source and sputtered ZnO:Al:N.

Table 1
FWHM, estimated grain size, carrier concentration and resistivity of the synthesized NZO films, sol–gel synthesised AZO, sol–gel produced ZnO:Al:N using NH_4Cl as source of nitrogen, sol–gel produced ZnO:Al:N using NH_4OH as source and sputtered ZnO:Al:N.

Sample	FWHM	Grain size (from XRD)	Carrier concentration (All the samples except ZnO:Al:N exhibited p-type doping) (/cm^3)	Resistivity (Ω cm)
NZO	0.0094	15.235 nm	1.76×10^{13}	246
ZnO:Al:N (sputtered)	NA	>100 nm cannot be estimated by Scherrer's formula	N/A (out of scale)	N/A (out of scale)
ZnO:Al:N (NH4Cl)	0.00854	16.88 nm	2.4×10^{16}	43
ZnO:Al:N (NH4OH)	0.00593	24.203 nm	4.35×10^{17}	20.4

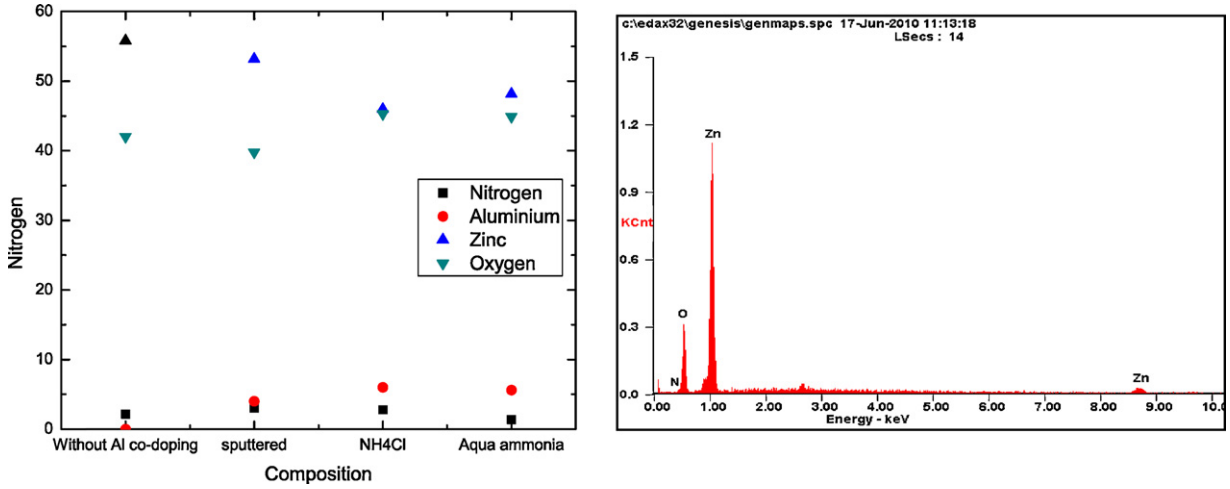

Fig. 3. EDS data of the synthesized NZO films, sol–gel synthesised AZO, sol–gel produced ZnO:Al:N using NH_4Cl as source of nitrogen, sol–gel produced ZnO:Al:N using NH_4OH as source and sputtered ZnO:Al:N and corresponding composition of the film.

solution is beneficial towards the formation of the P-type zinc oxide rather than acidic solution.

The Hall measurement (Table 1) tabulates the information of the p -type doping for all the films. It is shown that the p-type properties of sol–gel processed ZnO films are highly dependent on the nitrogen source. High resistivity was observed from the films without co-doping. The films co-doped with aluminium possess an acceptable resistivity with Hole concentration in the 10^{17} cm^{-3} and resistivity range between 45 and 62 cm^2/V s. These results correlate well with data published by Ge and Dutta [20,33].

Fig. 4 shows the Raman spectroscopy was obtained for NH_4Cl and NH_4OH NZO films. The peaks consist of several bands that can be attributed to Raman active phonon modes of wurtzite ZnO [42]. The E_2 (low) mode, located at around 100 cm^{-1} is out of the range of our spectra, which starts from around 260 cm^{-1}. In both peaks there is a broad peak at around 438 cm^{-1} that corresponds to the to E_2 (high) mode. The E_2 (high) is associated with oxygen atoms. The fact that no significant shift of the position can be observed for the E_2 (high) indicates the absence of strain [43]. Predominantly, one main peak is present at around 570 cm^{-1}. This peak corresponds to the *A*1 (LO) mode and is expected at 574 cm^{-1} [43]. Indeed, this peak is attributed to the nitrogen related defects. Kerr et al. [44] observed additional peaks at 280 and 570 cm^{-1}, as nitrogen dose is incorporated into ZnO films. Indeed, the peak was attributed to nitrogen related defects.

The optical properties of the sol–gel produced NZO were measured by the photoluminescence (PL) spectroscopy at room temperature. Fig. 5 illustrates the PL property of the NZO (without Al co-doping), NH_4Cl and NH_4OH NZO films. A broad peak centred at 380 nm (3.26 eV) in UV band can be observed in Fig. 5. The UV-emission is caused by the recombination of free excitons through exciton annihilation process. The addition of Al co-doping does not significantly alter the PL properties of the film. However, the selection of NH_4Cl as nitrogen dopant considerably alters the PL measurements and results in an addition peak at around 500 nm (green). The green band is attributed to oxygen vacancy defect centres [45]. These results correlate well with XRD data from Fig. 2. The PL measurements for NZO derived with NH_4Cl showed a broader XRD peak, which suggests an increasing disorder in the NZO film.

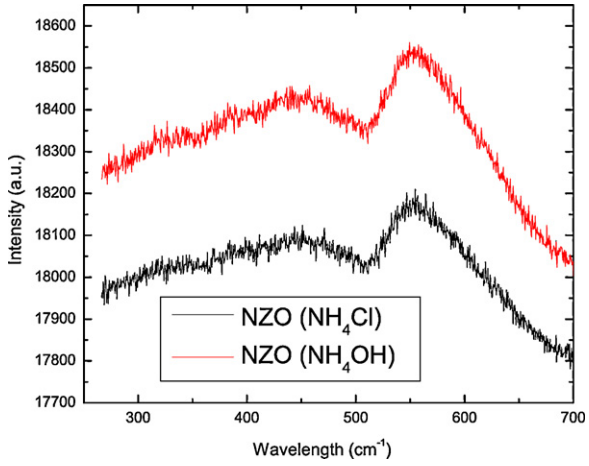

Fig. 4. Raman spectroscopy of ZnO:Al:N, with NH_4Cl (black) and NH_4OH as nitrogen source (red), showing the prominent peak at 570 cm^{-1}. (For interpretation of the references to colour in this figure legend, the reader is referred to the web version of the article.)

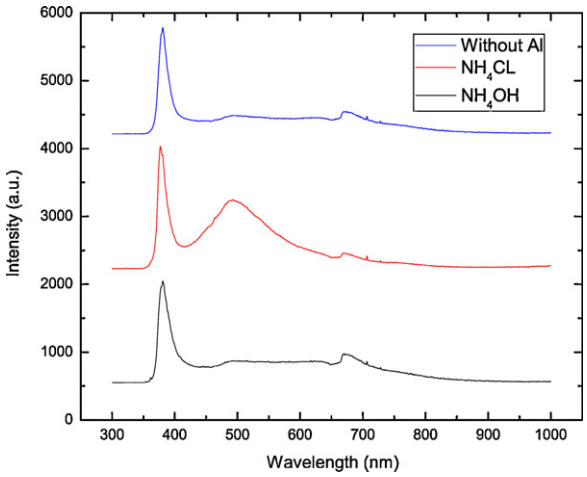

Fig. 5. Photoluminescence of ZnO:Al:N, with (a) NH_4OH, (b) NH_4Cl and (c) without Al co-doping.

4. Conclusions

The paper studies the effect of the nitrogen sources upon the formation of p-type ZnO films. In general, the hydroxide-based nitrogen sources are beneficial towards the formation of highly *c*-axis oriented ZnO:Al:N films. As confirmed by the XRD and Raman measurements, the structure enhancement, achieved by the formation of OH and NO, can produce excellent films. On the other hand, as observed from the PL measurements, the strong (green) emission from NZO (NH_4Cl) reveals the oxygen related vacancy and increased disorder. Further more, the Raman shift also confirms the incorporation of nitrogen into the films. These observations suggest that the mildly acidic chloride-based nitrogen sources, such as NH_4Cl, can produce extra HCl acid that etches the ZnO:Al:N films. It can therefore be concluded that the nitrogen sources can significantly affect the formation of p-type ZnO films and, as a result, change their opto-electrical properties.

Acknowledgements

The author I.Y.Y. Bu would like to thank National Science Council, under the grant NSC 98-2218-E-022-001 and NSC 99-2628-E-022-001 for financial support.

Appendix A. Supplementary data

Supplementary data associated with this article can be found, in the online version, at doi:10.1016/j.jallcom.2010.11.146.

References

[1] Ü. Özgür, Y.I. Alivov, C. Liu, A. Teke, M.A. Reshchikov, S. Do an, V. Avrutin, S.J. Cho, H. Morkoc, J. Appl. Phys. 98 (2005) 041301.
[2] P.C. Kao, S.Y. Chu, B.J. Li, J.W. Chang, H.H. Huang, Y.C. Fang, R.C. Chang, J. Alloys Compd. 467 (2009) 342–346.
[3] G. Meng, X.D. Fang, Y.K. Zhou, J. Seo, W.W. Dong, S. Hasegawa, H. Asahi, H. Tambo, M.G. Kong, L. Li, J. Alloys Compd. 491 (2010) 72–76.
[4] C.Y. Jiang, X.W. Sun, G.Q. Lo, D.L. Kwong, J.X. Wang, Appl. Phys. Lett. 90 (2007) 263501.
[5] L.C. Damonte, V. Donderis, S. Ferrari, J. Orozco, M.A. Hernandez-Fenollosa, J. Alloys Compd. 495 (2010) 432–435.
[6] K.D. Yuan, X. Yin, J.T. Li, J.J. Wu, Y.M. Wang, F.Q. Huang, J. Alloys Compd. 489 (2010) 694–699.
[7] C.D. Lokhande, P.M. Gondkar, R.S. Mane, V.R. Shinde, S.H. Han, J. Alloys Compd. 475 (2009) 304–311.
[8] Q. Wan, Q.H. Li, Y.J. Chen, T.H. Wang, X.L. He, J.P. Li, C.L. Lin, Appl. Phys. Lett. 84 (2004) 3654.
[9] M.W. Ahn, K.S. Park, J.H. Heo, J.G. Park, D.W. Kim, K.J. Choi, J.H. Lee, S.H. Hong, Appl. Phys. Lett. 93 (2008) 263103.
[10] A.J. Cheng, Y. Tzeng, Y. Zhou, M. Park, T. Wu, C. Shannon, D. Wang, W. Lee, Appl. Phys. Lett. 92 (2008) 092113.
[11] X.W. Sun, J.X. Wang, A. Wei, J. Mater. Sci. Technol. 24 (2008) 649–656.
[12] T.M. Barnes, K. Olson, C.A. Wolden, Appl. Phys. Lett. 86 (2005) 112112.
[13] W. Liu, F.X. Xiu, K. Sun, Y.H. Xie, K.L. Wang, Y. Wang, J. Zou, Z. Yang, J.L. Liu, J. Am. Chem. Soc. 132 (2010) 2498–2499.
[14] C.B. Tay, S.J. Chua, K.P. Loh, J. Phys. Chem. C 114 (2010) 9981–9987.
[15] Y.J. Zeng, Z.Z. Ye, W.Z. Xu, D.Y. Li, J.G. Lu, L.P. Zhu, B.H. Zhao, Appl. Phys. Lett. 88 (2009) 062107.
[16] S. Cho, Curr. Appl. Phys. 10 (2010) S443–S446.
[17] R. Qin, J.X. Zheng, J. Lu, L. Wang, L. Lai, G.F. Luo, J. Zhou, H. Li, Z.X. Gao, G.P. Li, W.N. Mei, J. Phys. Chem. C 113 (2009) 9541–9545.
[18] S.P. Wang, C.X. Shan, B.H. Li, J.Y. Zhang, B. Yao, D.Z. Shen, X.W. Fan, J. Cryst. Growth 311 (2009) 3577–3580.
[19] X.H. Pan, W. Guo, Z.Z. Ye, B. Liu, Y. Che, H.P. He, X.Q. Pan, J. Appl. Phys. 105 (2009) 113516.
[20] F. Zhu-Ge, Z.Z. Ye, L.P. Zhu, J.G. Lü, B.H. Zhao, J.Y. Huang, Z.H. Zhang, L. Wang, Z.G. Ji, J. Cryst. Growth 268 (2004) 163–168.
[21] C.P. Liu, G.R. Jeng, J. Alloys Compd. 468 (2009) 343–349.
[22] T. Ratana, P. Amornpitoksuk, S. Suwanboon, J. Alloys Compd. 470 (2009) 408–412.
[23] B. Wang, L.D. Tang, J.A. Qi, H.L. Du, Z.B. Zhang, J. Alloys Compd. 503 (2010) 436–438.
[24] T.T. Zhao, T. Yang, B. Yao, C.X. Cong, Y.R. Sui, G.Z. Xing, Y. Sun, S.C. Su, H. Zhu, D.Z. Shen, Thin Solid Films 518 (2010) 3289–3292.
[25] B. Xiang, P. Wang, X. Zhang, S.A. Dayeh, D.P.R. Aplin, C. Soci, D. Yu, D. Wang, Nano Lett. 7 (2007) 323–328.
[26] W.Z. Xu, Z.Z. Ye, Y.J. Zeng, L.P. Zhu, B.H. Zhao, L. Jiang, J.G. Lu, H.P. He, S.B. Zhang, Appl. Phys. Lett. 88 (2006) 173506.
[27] C. Ravichandran, G. Srinivasan, C. Lennon, S. Sivanathan, J. Kumar, Mater. Sci. Semicond. Process. 13 (2010) 46–50.
[28] H.C. Lu, J.L. Lu, C.Y. Lai, G.M. Wu, Physica B: Condensed Matter 404 (2009) 4846–4849.
[29] Y.R. Sui, B. Yao, J.H. Yang, H.F. Cui, X.M. Huang, T. Yang, L.L. Gao, R. Deng, D.Z. Shen, Appl. Surf. Sci. 256 (2010) 2726–2730.
[30] K.P. Bhuvana, J. Elanchezhiyan, N. Gopalakrishnan, T. Balasubramanian, J. Alloys Compd. 473 (2009) 534–537.
[31] D.C. Look, G.M. Renlund, R.H. Burgener, J.R. Sizelove, Appl. Phys. Lett. 85 (2004) 5269.
[32] I.S. Kim, E.K. Jeong, D.Y. Kim, M. Kumar, S.Y. Choi, Appl. Surf. Sci. 255 (2009) 4011–4014.
[33] M. Dutta, T. Ghosh, D. Basak, J. Electron. Mater. 38 (2009) 2335–2342.
[34] S.H. Yoon, D. Liu, D.N. Shen, M. Park, D.J. Kim, J. Mater. Sci. 43 (2008) 6177–6181.
[35] M. Copuroglu, L.H.K. Koh, S. O'Brien, G.M. Crean, J. Sol-Gel Sci. Technol. 52 (2009) 432–438.
[36] S.J. Kwon, J.H. Park, J.G. Park, Phys. Rev. E: Stat., Nonlinear Soft Matter Phys. 71 (2005) 11604.
[37] G. Srinivasan, J. Kumar, J. Cryst. Growth 310 (2008) 1841–1846.
[38] G.J. Fang, D. Li, B.L. Yao, Thin Solid Films 418 (2002) 156–162.
[39] V. Gupta, A. Mansingh, J. Appl. Phys. 80 (1996) 1063–1073.
[40] B.D. Cullity, Introduction to Magnetic Materials, Addison-Wesley, 1977.
[41] T. Tohsophon, J. Hüpkes, H. Siekmann, B. Rech, M. Schultheis, N. Sirikulrat, Thin Solid Films 516 (2008) 4628–4632.
[42] J. Serrano, A.H. Romero, F.J. Manjon, R. Lauck, M. Cardona, A. Rubio, Phys. Rev. B: Condens. Matter Mater. Phys. 69 (2004) 94306.
[43] B. Sieber, H. Liu, G. Piret, J. Laureyns, P. Roussel, B. Gelloz, S. Szunerits, R. Boukherroub, J. Phys. Chem. C 113 (2009) 13643–13650.
[44] L.L. Kerr, X. Li, M. Canepa, A.J. Sommer, Thin Solid Films 515 (2007) 5282–5286.
[45] K. Vanheusden, C.H. Seager, W.L. Warren, D.R. Tallant, J.A. Voigt, Appl. Phys. Lett. 68 (1996) 403.